Clinical, Cosmetic and Investigational Dentistry

Dovepress
Taylor & Francis Group

Open Access Full Text Article

ORIGINAL RESEARCH

In vitro Assessment of Open-Access Digital Workflow for Presurgical Nasoalveolar Molding in Unilateral Cleft Lip and Palate

Emily A Genovesi[1], Jessica E Canallatos[2], Laxmi Deepak Hulyalkar[1], Ridham V Varsani[1], Steven Makowka[3], Dany Atalla[4], Praveen Arany[1]

[1]Department of Oral Biology University at Buffalo, Buffalo, NY, USA; [2]Laurence C. Wright Craniofacial Center, Golisano Children's Hospital of Buffalo, Buffalo, NY, USA; [3]Materials Testing Core, University at Buffalo, Buffalo, NY, USA; [4]MeshDent Dental Automation Solution, Montreal, Quebec, Canada

Correspondence: Praveen Arany, Department of Oral Biology3435 Main Street, 553 BRB, University at Buffalo, Buffalo, NY, 14214, USA, Tel +1 716-829-3479, Fax +1 716-829-3942, Email prarany@buffalo.edu

Purpose: To evaluate digitally fabricated nasoalveolar molding (NAM) prostheses using open-source software against conventionally manufactured prostheses using an in vitro assessment of material mechanical properties, and fabrication efficiency.

Materials and Methods: Following IRB approval, a retrospective, in vitro comparative study was conducted using previously obtained, deidentified neonatal maxillary gypsum casts from patients with unilateral cleft lip and palate. NAM prostheses were fabricated using either conventional cold-cure acrylic resin or a digital workflow using open-access software (Meshmixer, Autodesk) and stereolithography 3D printing (Formlabs). Surface deviation relative to reference casts, fabrication time, flexural strength, flexural modulus, and microscopic structural analysis of 3D printed resin versus conventional materials were evaluated.

Results: Digital NAM prostheses demonstrated significantly ($n = 17$, $p = 0.038$) reduced surface cast-based deviation compared to conventional prostheses (mean deviation: 1.53 ± 0.19 mm vs. 1.69 ± 0.25 mm), reflecting nearly 10% improvement in fit relative to the reference cast with the digital method. Materials analysis revealed that 3D-printed resin blocks of standardized testing dimension demonstrated significantly higher flexural strength ($n = 7$, $p < 0.0001$) at 67.17 ± 4.8 MPa compared to conventional acrylic blocks at 28.7 ± 3.32 MPa. Flexural modulus was also significantly ($n = 7$, $p < 0.0001$) different between groups, with values of 1713 ± 131.6 MPa for 3D printed resin and 797.5 ± 99.0 MPa for conventional acrylic, indicating greater stiffness in the 3D printed resin material. Microscopic analysis revealed a uniform, void-free structure in 3D printed resin blocks in contrast to visible air entrapment in conventional cold-cure acrylic blocks.

Conclusion: Within the limitations of this in-vitro study using gypsum casts as a reference standard, this work validates a digital workflow for NAM prosthesis fabrication using freely available open-source software (Meshmixer). By providing a reproducible, cost-free workflow, this study offers a practical guide for clinicians initiating digital NAM design and future sequential treatments, supporting wider accessibility and precision in presurgical NAM therapy, particularly in resource-limited settings.

Keywords: nasoalveolar molding, cleft lip and palate, additive manufacturing, 3d printing, digital workflow, open access, Meshmixer, CAD/CAM

Introduction

Cleft lip and palate (CLP) are among the most common congenital craniofacial anomalies, affecting approximately 1 in 1050 live births worldwide.[1–4] These defects result from failed fusion of the maxillary and nasal prominences during early embryonic development and require coordinated multidisciplinary care to address feeding, speech, hearing, growth, and psychosocial challenges. Comprehensive management typically involves integrated craniofacial teams including pediatrics, dentistry, otolaryngology, speech pathology, orthodontics, prosthodontics, and reconstructive surgery.[5] Presurgical infant orthopedic (PSIO) therapies have been developed to improve surgical and functional outcomes. Among them, nasoalveolar molding (NAM) has become a widely adopted adjunct since its introduction in the

https://doi.org/10.2147/CCIDE.S588444
Received: 27 December 2025
Accepted: 6 April 2026
Published: 23 April 2026

1990s.[6–11] Owing to neonatal cartilage plasticity influenced by maternal estrogen–related hyaluronic acid, NAM begun within the first weeks of life can gradually align cleft segments and improve nasal symmetry before primary lip repair, usually performed at two weeks to the first three months of age.[12] Clinical studies indicate that NAM can reduce cleft severity, enhance nasolabial esthetics, and decrease the need for secondary surgical revisions.[13,14]

Despite these benefits, conventional NAM fabrication remains labor intensive and operator dependent with overall increased burden of care on both patients and providers.[15,16] Traditional appliances are fabricated manually from acrylic resin on gypsum casts derived from neonatal impressions affording a multi-step process requiring significant technical expertise, multiple laboratory procedures, and considerable time. Treatment also demands frequent clinical adjustments and follow-up visits, which can impose substantial logistical and financial burdens on families, including travel costs, missed work, and lost income.[17,18] These factors collectively limit accessibility, particularly in resource-constrained regions. Digital technologies such as intraoral scanning, computer-aided design (CAD), and additive manufacturing have emerged as promising alternatives to simplify NAM production and improve precision.[19–22] Digital NAM workflows allow virtual appliance design and three-dimensional (3D) printing, shortening fabrication time and reducing material variability while eliminating risks associated with neonatal impressions.[23,24] Clinical reports and systematic reviews suggest that digital NAM achieves outcomes comparable to conventional methods, with additional benefits including safer data acquisition, faster reproduction, and improved predictability through virtual simulation of segment movement.[23–26]

However, most current digital NAM workflows rely on proprietary CAD platforms (eg, Exocad, 3Shape, Rhino-based systems) that require paid licenses, dedicated hardware, and technical expertise.[27–31] The cost of these systems can be prohibitive in smaller clinics and low-resource environments, limiting the broader adoption of digital methods. A few studies have reported digital NAM fabrication using commercial software, but open-access workflows remain under-explored. Among available free tools, Autodesk MeshMixer is a cost-free mesh-editing and modeling program widely used in dentistry for tasks such as trimming digital impressions and preparing files for 3D printing. Despite its popularity, there are few detailed reports describing complete NAM design workflows using MeshMixer. Demonstrating the feasibility of such a process is important, as its free access, modest hardware requirements, and active user community would significantly improve access of digital NAMs.

This study was aimed at specifically addressing this gap by evaluating a complete digital NAM fabrication workflow using open-source design software (Autodesk MeshMixer) and stereolithography-based 3D printing (Formlabs Form 3). We hypothesized that the digital workflow could produce NAM prostheses with surface adaptation comparable to conventionally fabricated plates, while offering improved accessibility, reproducibility and process efficiency (time and costs). To evaluate specific concerns of the change from current clinical workflow, this study compared the digital approach with conventional NAM fabrication through both qualitative and quantitative assessments. The primary outcome assessed surface deviation following iterative closest point (ICP) alignment, serving as an objective measure of prosthesis to cast adaptation. Secondary outcomes included workflow feasibility and comparative analysis of fabrication efficiency. Demonstrating this feasibility may help lower the technical and financial barriers to digital NAM adoption in diverse clinical environments.

Methods

Study Design and Sample Selection

This investigation was conducted as an in vitro laboratory study utilizing retrospectively collected clinical casts. Ethical approval for this in vitro study was obtained from the University at Buffalo Institutional Review Board in conjunction with the Erie County Medical Center (ECMC) Office of Research Compliance (IRB Protocol #7405 approved 2023) prior to initiation of the study. This investigation was designed as an exploratory early feasibility study based on the finite number of archival unilateral cleft casts available in the institutional records during the study period. Accordingly, no a priori formal sample size or power calculation was performed; instead, all eligible casts meeting the inclusion criteria were included. Seventeen de-identified neonatal maxillary gypsum casts from patients with unilateral cleft lip and palate (UCLP) were obtained from the archival records of the ECMC Department of Oral Oncology and Maxillofacial

Prosthetics. Clinical casts were originally obtained in the craniofacial clinic during the period January 2022 to June 2023 from clinical impressions taken prior to initiation of nasoalveolar molding (NAM) therapy at approximately two weeks of age. All laboratory fabrication and analysis for the present in vitro study were conducted between July 2023 and June 2024. Each cast served as the anatomical reference for fabrication of one conventional and one digital NAM, allowing direct comparison of the two fabrication techniques derived from the same underlying anatomy. In total, 17 conventional and 17 digital prostheses (34 appliances) were analyzed that included fifteen left-sided clefts and two right-sided clefts casts. Additional digital prostheses were generated from repeated workflows for several casts to qualitatively evaluate the consistency of the digital fabrication protocol.

Conventional NAM Fabrication

Conventional NAM prostheses were fabricated using established clinical laboratory protocols previously described for presurgical infant orthopedics (Figure 1A–I).[32] All conventional acrylic NAM prostheses were fabricated by an experienced dental laboratory technician who did not participate in the digital design workflow. Palatal undercuts were relieved using block-out putty (Great Lakes Dental, Lab Putty and Catalyst Kit, 100–075) to facilitate insertion and removal of the prosthesis. Autopolymerizing acrylic resin (Biocryl ICE Acrylic Kit, Great Lakes Dental Technologies, Tonawanda, NY, USA) was applied using the salt-and-pepper technique, in which polymer powder and monomer liquid are sequentially applied to the cast until the desired appliance thickness is achieved. Polymerization was performed under pressure according to manufacturer recommendations. Following cold-cure polymerization, prostheses were finished and polished using acrylic rotary burs and pumice slurry to obtain smooth surfaces. Completed prostheses were digitized using a 3Shape E4 desktop scanner (3Shape, Copenhagen, Denmark) with a scanning resolution of approximately 50 µm, generating Standard Tessellation Language (STL) surface files for digital analysis.

Digital NAM Fabrication Workflow

The digital fabrication workflow began with scanning the same gypsum casts using the 3Shape E4 desktop laboratory scanner, producing high-resolution STL files (Figure 2A–F). A detailed step-wise outline of the digital fabrication workflow (Supplemental Figures 1 and 2). Briefly, the digital files were imported into Meshmixer (Autodesk, San Rafael, CA, USA) for virtual prosthesis design (Figure 3A). This software was specifically selected as an open access primary design platform that provides robust mesh editing tools suitable for constructing and modifying intraoral prostheses, thereby supporting an open-access workflow replicable in diverse clinical environments. Digital prosthesis design followed a standardized workflow consisting of model orientation and preparation (Figure 3B). Mesh refinement and artifact removal, including trimming extraneous geometry and repairing surface irregularities of digitized gypsum casts using Meshmixer analysis and smoothing tools (Figure 3C). Identification and digital block-out of anatomical undercuts was performed using sculpting tools to create relief in areas that would otherwise impede prosthesis insertion and removal (Figure 3D). Undercut relief was applied with an approximate offset of 0.5–1.0 mm in the palatal undercut regions. Generation of the prosthesis shell created using offset and extrusion functions to produce a uniform appliance thickness of approximately 2.0 mm (Figure 3E). Surface smoothing and inspection were performed to ensure continuity of the prosthesis surface and absence of mesh defects and additional accessories like button and vent were added (Figure 3F). All digital prosthesis designs were performed by a single trained operator following a standardized protocol to minimize inter-operator variability. Completed prosthesis designs were exported as STL files and imported into the free software PreForm (Formlabs, Somerville, MA, USA) for print preparation, 3D printed support generation, and build-orientation optimization.

Additive Manufacturing and Post-Processing

Digital prostheses were fabricated using a Stereolithography 3D printer (Form 3, Formlabs, Somerville, MA, USA). The Form 3 SLA printer was chosen because it is widely used for its ability to generate high-resolution printing with biocompatible photopolymer resins. Prostheses were printed using Dental LT Clear resin (Formlabs), an FDA-cleared, long-term intraoral material that has been validated for occlusal splints and intraoral appliances, thereby providing a clinically relevant material for NAM-like devices in this experimental setting. Printing parameters included a 25-µm

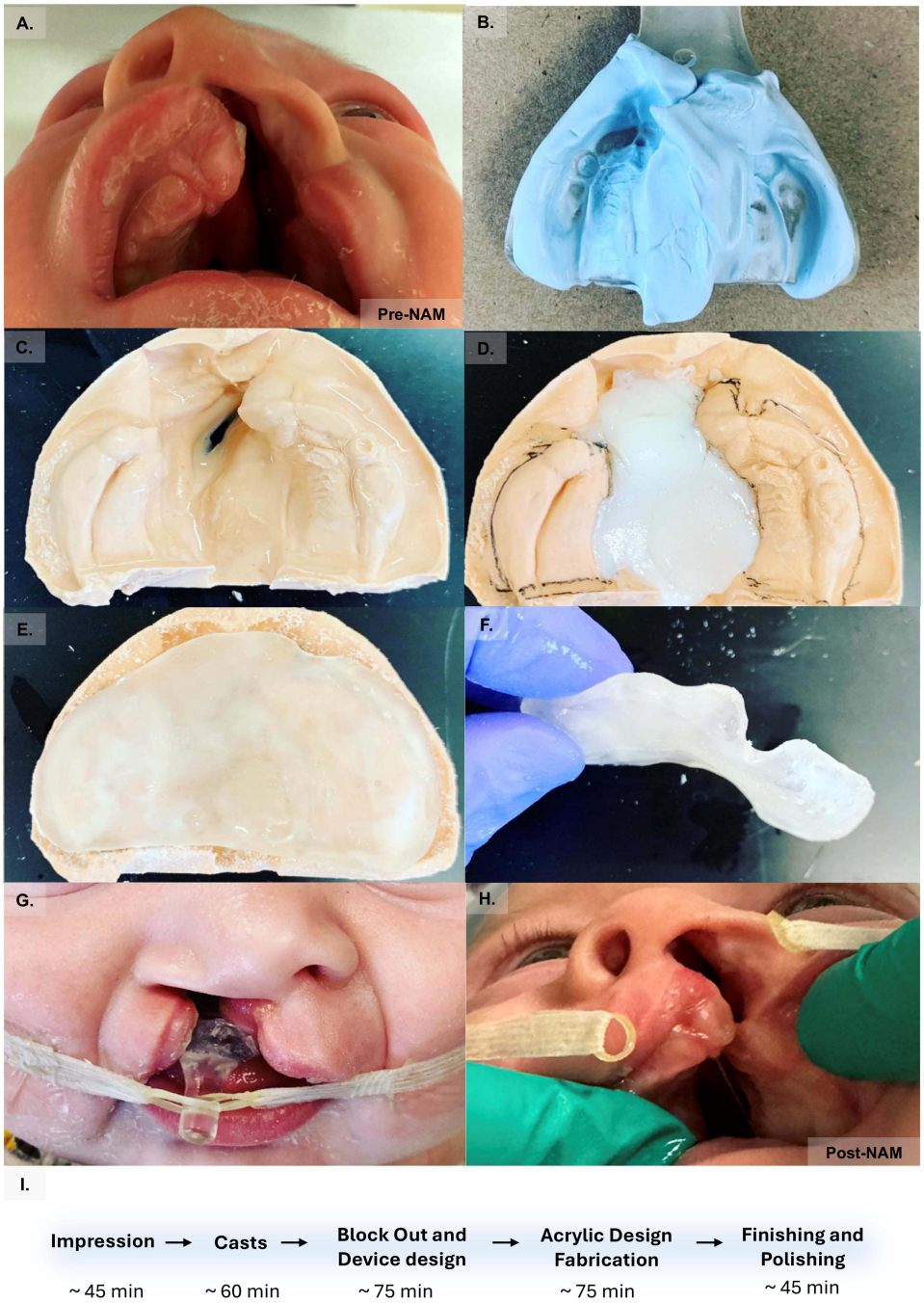

Figure 1 Conventional workflow to fabricate NAM prosthesis (**A**) clinical image prior to NAM treatment (**B**) taking an alginate impression of the area (**C**) generating a gypsum cast (**D**) Cleft palate block out (**E**) generating the base plate for the prosthesis (**F**) finishing and polishing the acrylic prosthesis (**G**) clinical image of NAM fitted with clinical tape and elastics on retention button (**H**) clinical image post-NAM treatment (**I**) procedural steps and estimated time for conventional workflow.

layer thickness and optimized print orientation to minimize support contact with intaglio surfaces. Following printing, prostheses underwent standardized post-processing according to manufacturer guidelines. Printed components were washed in 99% isopropyl alcohol for 20 minutes using a Form Wash system to remove uncured resin. After air-drying for approximately 30 minutes, prostheses were post-cured at 60°C for 60 minutes under 405 nm ultraviolet light using a curing unit (Form Cure, Formlabs) to achieve optimal material properties. Support structures were removed and contact points were smoothed using fine abrasive instruments. Completed prostheses underwent visual inspection to confirm structural integrity and surface quality prior to analysis.

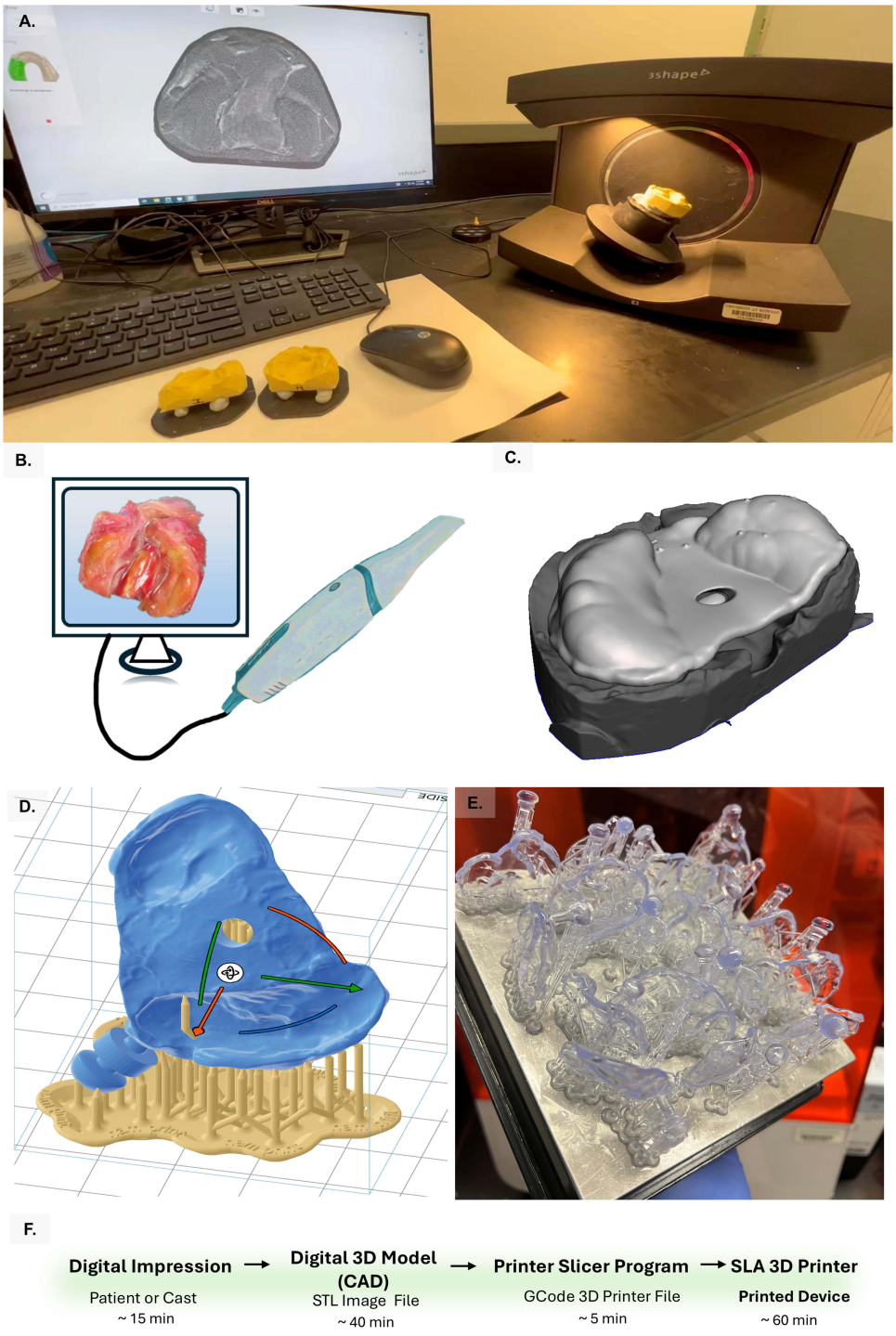

Figure 2 Digital workflow to fabricate NAM prosthesis (**A**) Indirect technique using a desktop scanner (3Shape, desktop E4 scanner) (**B**) alternate method for fully digital workflow using intraoral scan to capture cleft palatal anatomy (**C**) digital model of the prosthesis in Meshmixer (**D**) model preparation for 3D printing manufacturing using PreForm slicer program (STL to GCode), the red and green arrows indicate axis of rotations (**E**) 3D printed NAMs using FormLabs Form3 stereolithography printing (**F**) procedural steps and estimated time for digital workflow steps.

Surface Deviation Analysis

Three-dimensional surface comparisons were performed using CloudCompare software (version 2.12.4, EDF R&D, Telecom ParisTech, France) (Supplemental Figure 3). Surface alignment between digital models was achieved using the Iterative Closest Point (ICP) algorithm, which iteratively minimizes spatial discrepancy between two meshes by

https://doi.org/10.2147/CCIDE.S588444

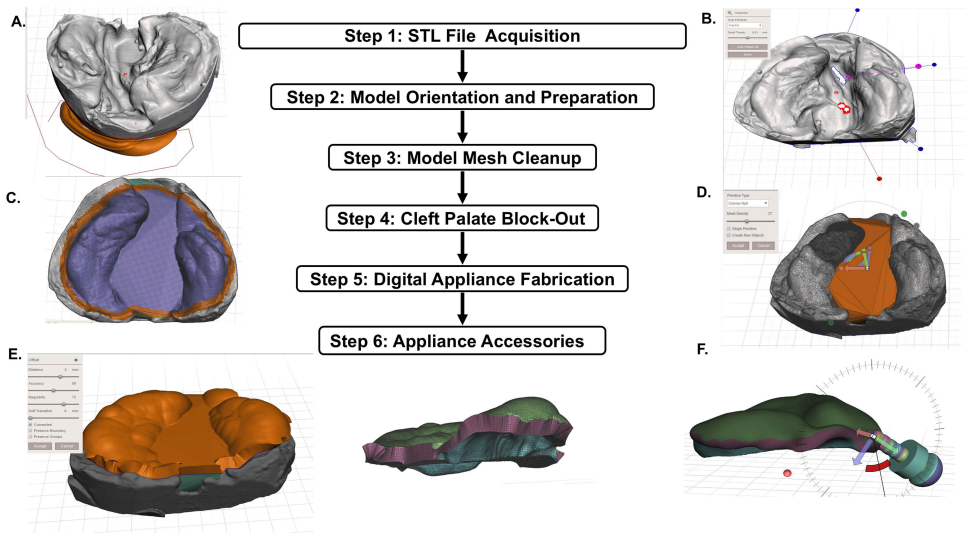

Figure 3 Stepwise methodology for digital fabrication of NAM plates using Meshmixer. The image in the center outlines each step to generate the prosthesis. (**A**) Acquisition of the digital file in Meshmixer software (**B**) Model is oriented and prepared for digital manipulation (**C**) Model is refined by removing artefactual defects, smoothened boundaries and defects are clearly isolated and outlined (**D**) The cleft space is blocked out to begin simulating the prosthesis foundation (**E**) The base is extended and forms the initial prosthesis that is further refined into final prosthesis format as shown in image on left, the lateral profile is outlined in the right image (**F**) Accessories like retention button and central vent are added prior to finalizing prosthesis and 3D printing. A detailed workflow with each of these steps is outlined in the Supplemental Materials.

identifying the closest point correspondences across surfaces and applying rotational and translational transformations until convergence criteria are met. Prior to experimental analysis, the alignment protocol was validated using identical digital models of a standard coin (US Penny) of known dimension to confirm that the ICP algorithm produced negligible deviation under ideal conditions (Supplemental Figure 4). For each cast, a cast-to-prosthesis comparison was performed in which the internal (*intaglio*) surface of the NAM appliance was aligned to the corresponding maxillary cast. Following ICP registration, deviation values were calculated as point-to-surface distances from the intaglio surface of the prosthesis to the reference cast across the entire basal seat region, excluding peripheral areas beyond the vestibular reflection. Mean absolute deviation and standard deviation were extracted from CloudCompare output for each prosthesis and used as the primary trueness metric for statistical analysis. Deviation values were calculated as point-to-surface distances across the intaglio surface of each prosthesis. Deviation maps were visualized using standardized color scales representing the magnitude and direction of deviation. Mean deviation values and standard deviations were extracted directly from the CloudCompare output for statistical analysis. Surface analysis was performed by an independent investigator who was blinded to the fabrication method of each prosthesis to minimize analytical bias.

Materials Analysis and Mechanical Testing

Mechanical testing was performed to compare flexural properties of the materials used for conventional and digitally fabricated prostheses. Specimens of conventional acrylic and 3D-printed resin were fabricated and tested according to ASTM D790-17 standards for flexural testing of polymeric materials, using a three-point bending configuration on a universal testing machine. Rectangular specimens were prepared with standardized dimensions of 2 mm thickness, 45 mm length, and 12.7 mm width. Seven specimens were fabricated for each material group (n = 7 per group). Flexural strength and modulus of elasticity were measured using a universal testing machine under three-point bending conditions. Material cross-sections were examined using a stereomicroscope (Nikon) to qualitatively evaluate internal material structure, including the presence of voids, air entrapment, or structural irregularities. Digital images were captured; contrast and brightness were adjusted uniformly to maintain consistent visualization.

Statistical Analysis

Statistical analyses were performed using GraphPad Prism (v10.4.0, Boston, MA). Data normality was assessed using the Shapiro–Wilk test. For group comparisons, unpaired *T*-tests with Welch's correction were used for all continuous outcomes (flexural modulus and strength) while surface deviation analyses was performed pairwise between the conventional and digital prostheses corresponding to the same cast. Statistical significance was defined as $p < 0.05$.

Results

Surface Deviation Analysis

Surface deviation analysis demonstrated measurable differences between conventional and digitally fabricated NAM prostheses (Figure 3A–F). When aligned to their respective reference casts using iterative closest point (ICP) registration, conventional acrylic NAM prostheses exhibited a mean surface deviation of 1.69 ± 0.25 mm, whereas digitally fabricated prostheses demonstrated a mean deviation of 1.53 ± 0.19 mm (Figure 4A–C). This difference was statistically significant ($n = 17$ specimens per group, $p = 0.038$), representing approximately 10% lower mean deviation for digitally fabricated prostheses. Deviation magnitudes were interpreted according to clinically relevant tolerance thresholds for prosthesis adaptation: Excellent fit: ± 0.2 mm deviation; Acceptable fit: ± 0.5 mm deviation; Poor fit: >± 1.0 mm deviation. For descriptive purposes, deviation magnitudes were grouped into conceptual categories for prosthesis adaptation. These ranges were selected to provide an intuitive framework for interpreting millimeter-scale gap values in this in-vitro model, drawing on general prosthodontic literature that emphasizes sub-millimetric marginal and internal gaps as desirable for fixed restorations, although no NAM-specific thresholds have been established.

Mechanical Properties

Mechanical testing demonstrated distinct differences between materials used for conventional and digitally fabricated prostheses (Figure 4D). Three-point flexural testing revealed that the 3D-printed resin specimens (Formlabs Dental LT Clear) exhibited significantly greater flexural strength, with a mean value of 67.17 ± 4.8 MPa, compared to 28.70 ± 3.32 MPa for conventional cold-cure acrylic specimens (Biocryl ICE acrylic) ($n = 7$ per group, $p < 0.0001$) (Figure 4E). Moreover, flexural modulus was also higher in the 3D-printed resin specimens (1713 ± 131.6 MPa) than conventional acrylic specimens (797.5 ± 99.0 MPa) ($p < 0.0001$) (Figure 4F). This suggests that the digitally fabricated NAMs were stiffer and more resilient.

Microscopic Analysis

Microscopic evaluation of material cross-sections demonstrated qualitative structural differences between conventional acrylic and 3D-printed resin materials (Figure 4G–H). Conventional cold-cure acrylic specimens exhibited heterogeneous internal structures, including visible voids and opaque regions consistent with air entrapment during manual mixing and polymerization. 3D-printed resin specimens demonstrated uniform, homogenous internal structures, without visible voids or air bubbles under light microscopy.

Discussion

This study demonstrates the feasibility of an open-access digital workflow for fabrication of nasoalveolar molding (NAM) prostheses using freely available design software and stereolithographic (SLA) additive manufacturing. Accordingly, the interpretation of these findings is intentionally limited to in vitro outcomes such as cast-based surface adaptation, material mechanical behavior, and fabrication efficiency, without inferring direct clinical effects on NAM treatment results. Within the limitations of this in vitro investigation, digitally fabricated NAM prostheses demonstrated lower mean surface deviation relative to conventionally fabricated acrylic devices. Deviation maps visualized through color-coded heat maps revealed distinct surface adaptation patterns. Conventional prostheses frequently demonstrated localized over-contouring or under-contouring in palatal regions, particularly along the alveolar ridge and cleft margins. In contrast, digitally fabricated prostheses exhibited more uniform surface adaptation patterns, reflecting greater

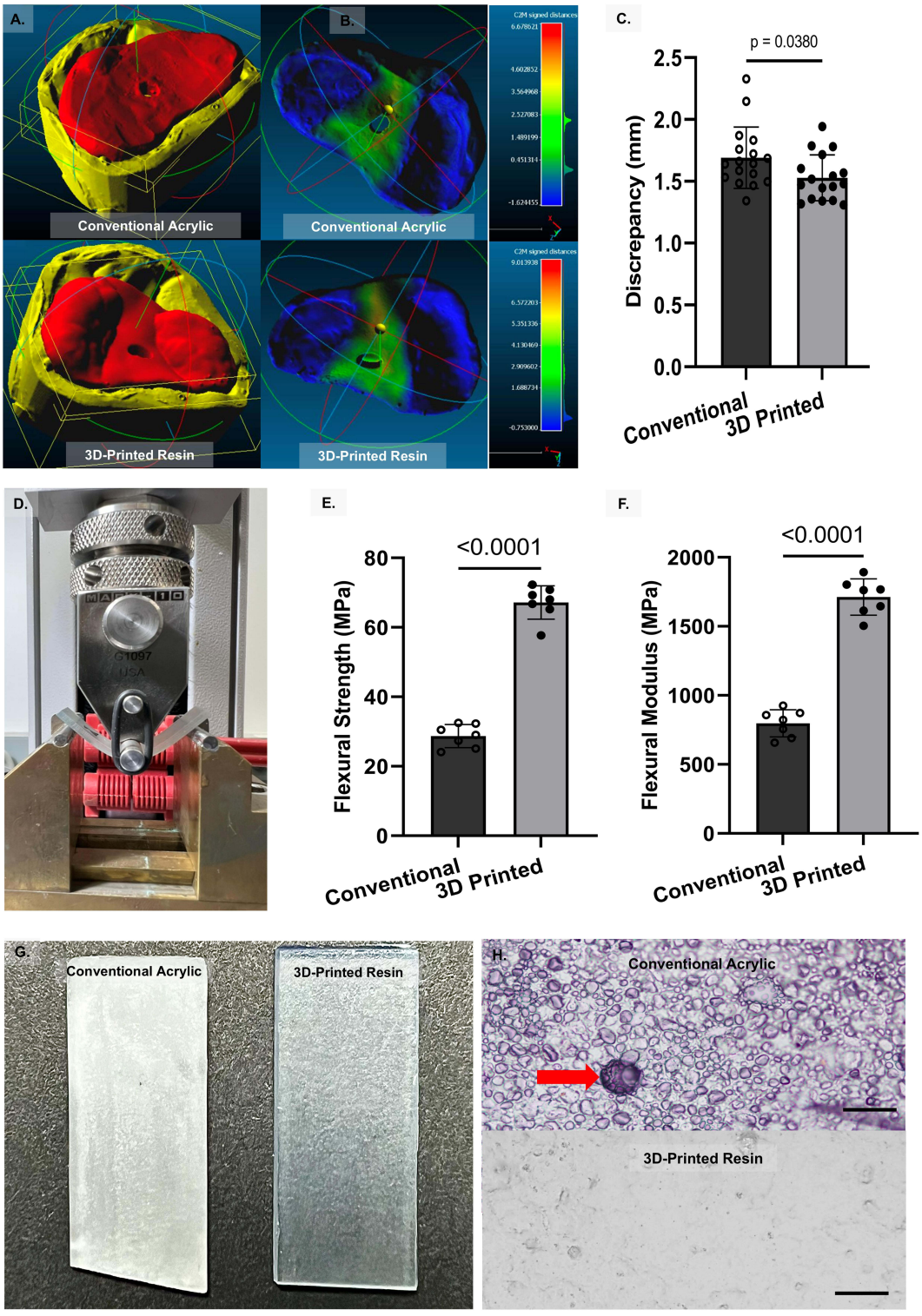

Figure 4 Comparative analysis of conventional and digital NAMs. (**A**) Example of a patient cast used to generate conventional acrylic prosthesis (top) and a 3D printed digitally fabricated NAM prosthesis (bottom) that were overlaid on the reference cast (yellow). (**B**) Conventional acrylic NAM (top) and digital NAM prosthesis (bottom) showing intaglio surfaces of both NAM plates. A heat map gradient shows accuracy of fit with blue being most accurate while green, yellow, red being progressively less. (**C**) Quantitative analysis of surface discrepancies was performed and analyzed for statistical significance (n = 17, p = 0.00380) (**D**) Mechanical characterization of standardized sample block using a universal testing machine for 3-point flexural strength and modulus was performed (**E**) Flexural strength among conventional and 3D printed blocks were analyzed (n = 7, p < 0.0001) (**F**) Flexural modulus among conventional and 3D printed blocks were analyzed (n = 7, p < 0.0001) (**G**) Digital images were assessed for material translucency among conventional cold cure acrylic (left) and a SLA 3D printed resin block (**H**) Phase microcopy of the cold cure acrylic block (top) noted voids (red arow) and trapped spaces in conventional block with higher opacity than the more homogenous SLA 3D printed resin sample (bottom). Scale bar = 100 uM.

https://doi.org/10.2147/CCIDE.S588444

consistency of the digitally designed geometry. Deviation thresholds are consistent with previously reported prosthodontic and digital dentistry tolerance ranges for intraoral prosthetic adaptation.

The differences observed in surface deviation may reflect advantages inherent to digital design and additive manufacturing workflows. Internal adaptation influences how securely a NAM plate seats on the palate and how molding forces are transmitted to soft tissues and alveolar segments; therefore, lower cast-based surface deviation in this in-vitro model is interpreted as improved trueness of fit with potential relevance for prosthesis retention and tissue loading, although these clinical outcomes were not directly measured here. In conventional fabrication, multiple manual steps including block-out of undercuts, acrylic adaptation, and polymerization may introduce variability during prosthesis formation. In contrast, digital workflows allow prosthesis geometry to be defined precisely within the computer-aided design (CAD) environment and reproduced consistently through additive manufacturing. However, it should be acknowledged that improved adaptation observed in this study cannot be attributed solely to elimination of manual steps. Other factors including scanner accuracy, CAD operator technique, and printer resolution may also influence the final prosthesis geometry and surface adaptation. As such, the apparent advantages of the digital workflow should be interpreted as hypothesis-generating and not as definitive evidence that removal of manual steps is the primary driver of improved fit.

Evaluation of prosthesis fit in digital dentistry is commonly conceptualized within the framework of trueness and precision, as defined by ISO standards. Trueness refers to the deviation of a manufactured object from the reference geometry, while precision reflects repeatability across repeated fabrications. Previous CAD/CAM prosthodontic investigations have assessed both parameters using three-dimensional inspection software to quantify deviation across multiple manufacturing methods.[33] The present study primarily evaluated trueness by comparing prosthesis geometry to the originating cast using surface deviation analysis. Future studies incorporating repeated digital fabrications could further evaluate precision and reproducibility of the proposed workflow. Virtual surface deviation analysis using 3D inspection software has become a widely accepted method for evaluating prosthetic adaptation. Nevertheless, complementary approaches for assessing actual physical gaps, such as the silicone replica technique, have been used extensively in prosthodontic research to measure marginal and internal fit under digital microscopy.[34] Incorporation of such physical validation methods may further strengthen future investigations comparing digital and conventional NAM fabrication techniques.

Mechanical testing revealed that the SLA 3D-printed resin exhibited statistically higher flexural strength and flexural modulus compared with conventional acrylic, indicating greater resistance to bending forces and increased stiffness under standardized test conditions. While these findings confirm that the printed resin is mechanically stronger and stiffer in vitro, the clinical relevance of these differences remains uncertain. In practice, forces applied during normal NAM use are likely lower than those used in laboratory testing, and both materials are expected to provide sufficient strength without compromising tissue safety. Increased strength and stiffness may reduce the risk of accidental fracture but could also alter force transmission to oral tissues; clinical studies are needed to determine how these material properties affect appliance durability, patient comfort, and overall efficacy during NAM therapy.

These structural irregularities identified through light microcopy of the conventional acrylic are consistent with previously described limitations of manually fabricated acrylic prostheses. The layer-by-layer polymerization process used in stereolithography manufacturing likely contributed to the more consistent internal material structure observed. These qualitative observations may partially explain the higher flexural strength observed in the SLA resin specimens. In addition to fabrication accuracy, digital workflows offer potential advantages in terms of efficiency and reproducibility. In the present study, observational timing during protocol development suggested that digital prostheses could be fabricated in substantially less operator-intensive time than conventional laboratory procedures, largely because many manual steps (acrylic mixing, adaptation, and finishing) are replaced by automated printing and post-processing. It is important to emphasize that these measurements were descriptive and not obtained through a formal time-motion analysis, they should be interpreted qualitatively rather than as definitive evidence of a specific percentage reduction in fabrication time.

Similarly, caregiver adherence and parental burden during NAM therapy represent important clinical considerations, as prior studies have highlighted the cumulative impact of repeated clinic visits, travel time, and lost income on families undergoing NAM treatment. While the digital workflow evaluated in this in-vitro study primarily targets laboratory-side efficiency and does not directly alter the number of scheduled clinical visits, it may offer provider-level advantages, such

as reduced technician time for manual acrylic processing, the ability to rapidly reproduce or replace appliances from stored design files, and the potential to integrate remote or distributed manufacturing models in future clinical applications that could ultimately help reduce aspects of caregiver burden or improve compliance. However, the present study did not measure financial costs, visit frequency, or caregiver-reported outcomes, and any potential reductions in travel-related expenses or loss of income remain speculative. Consequently, the impact of digital NAM workflows on patient-level and family-level costs should be regarded as hypothesis-generating and will require prospective clinical evaluation.

A notable aspect of the present workflow is the use of open-access CAD software. Many previously reported digital NAM protocols rely on proprietary software platforms that can present significant financial barriers, particularly in resource-limited healthcare environments.[35,36] By contrast, freely available software such as Meshmixer provides robust mesh editing capabilities and integration with standard stereolithography printing workflows. The use of accessible design tools may therefore facilitate broader adoption of digital NAM fabrication approaches across institutions with varying technological resources.

Limitations of Current Study

Several limitations should be considered when interpreting the results of this study. First, this investigation was conducted in-vitro using deidentified neonatal casts and therefore does not directly assess clinical performance of the prostheses in patients. Improved surface adaptation on casts does not necessarily translate to improved intraoral retention, tissue response, or treatment outcomes during NAM therapy. Second, the sample size consisted of seventeen casts. While this is typical for early feasibility studies, it limits statistical power to detect smaller differences and constrains generalizability. Future studies with larger, prospectively determined samples will be required to confirm these findings. Third, the study relied on virtual surface deviation analysis to evaluate prosthesis adaptation. Although this approach allows detailed three-dimensional comparison of prosthesis geometry, it does not directly measure internal gaps under clinical loading conditions. Complementary validation methods, such as silicone replica analysis, may provide additional insight into the physical adaptation of prostheses. Finally, digital fabrication requires access to scanning and additive manufacturing technologies. While these tools are becoming increasingly available, variability in equipment availability, material costs, and institutional infrastructure may influence the feasibility of implementing digital NAM workflows in some clinical settings. Moreover, like conventional NAM, CAD/CAM-based NAM remains dependent on frequent follow-up, specialized clinical teams, and caregiver adherence, and the present in-vitro findings do not yet address these shared limitations at the patient-care level.

Future Research Directions

Future investigations should focus on prospective clinical comparisons between digitally fabricated and conventionally fabricated NAM prostheses. Important outcome measures include cleft gap reduction, nasal symmetry improvement, treatment duration, appliance retention, and caregiver-reported satisfaction. Additional work is also needed to evaluate precision and reproducibility of digital NAM fabrication through repeated appliance production from identical datasets. Integration of complementary validation methods, such as silicone replica analysis, may further strengthen assessment of prosthesis adaptation.[37,38] Advances in digital dentistry also create opportunities to explore fully digital clinical workflows, including directly intraoral scanning of neonatal arches to eliminate conventional impression procedures. Such approaches could potentially reduce patient discomfort and streamline clinical processes. Finally, emerging research in computational design and artificial intelligence may enable automated treatment planning systems capable of generating sequential NAM prostheses based on initial patient anatomy (Figure 5A–C). This workflow has been well validated with tooth aligners and could be extended here to CLCP care via these digitally fabricated NAMs. Although these technologies remain in early stages of development, they represent a promising direction for future research aimed at improving efficiency, accessibility, and personalization of presurgical infant orthopedic therapies.

- We recognize that this study focuses on the digital adaptation of the intraoral plate component; future research will incorporate the nasal stent into the design of subsequent appliances.

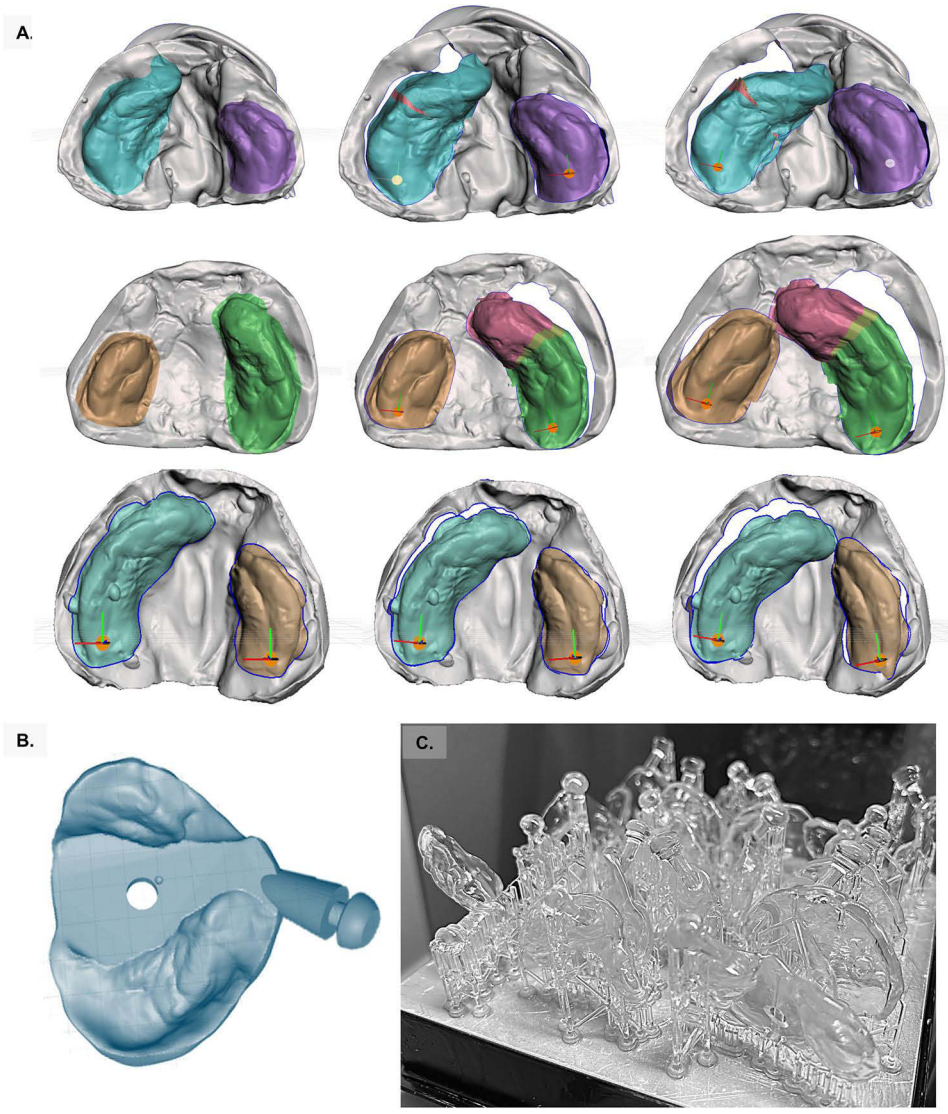

Figure 5 Concurrently printed Digital NAMs for sequential future treatments (**A**) Simulated representation of three cases where progressive extrapolation of desired nasoalveolar arches can be envisioned (**B**) Prosthesis design file for NAM with retention button (**C**) Series of NAM prostheses fabricated generated with SLA 3D printing as per projected anatomy.

Conclusions

Within the limitations of this in vitro investigation, digitally fabricated NAM prostheses produced using open-access design software and stereolithographic printing demonstrated lower mean surface deviation and reduced fabrication time compared with conventional acrylic prostheses. Mechanical testing indicated that the printed resin material exhibited greater flexural strength and stiffness relative to cold-cure acrylic. While these findings support the technical feasibility of an open-access digital NAM workflow, clinical studies are required to determine whether these differences translate to reduced burden of care and improved treatment outcomes in patients with unilateral cleft lip and palate.

Ethics Statement

This study was conducted using deidentified neonatal maxillary gypsum casts and was approved by the institutional review board (IRB #7405) at Erie County Medical Center for development of the digital workflow. The research was conducted in accordance with the Declaration of Helsinki and Good Clinical Practice guidelines. No direct patient involvement was required for this in vitro comparative analysis.

Acknowledgments

We would like to thank Dr. Michael Markiewicz, Oral Maxillofacial Surgery, University at Buffalo School of Dental Medicine for the Student Dental Research Award (EG), and University faculty funds (PRA) for enabling this research.

Disclosure

The authors declared no potential conflicts of interest with respect to the research, authorship, and/or publication of this article.

References

1. Allam E, Stone C. Cleft lip and palate: etiology, epidemiology, preventive and intervention strategies. *Global Health Perspectives*. 2013.
2. Zhou X, Jiang Y, Fang J, et al. Incidence of cleft lip and palate and epidemiology of perinatal deaths related to cleft lip and palate in Hunan Province, China, 2016–2020. *Sci Rep*. 2023;13(1):10304. doi:10.1038/s41598-023-37436-y
3. Salari N, Darvishi N, Heydari M, et al. Global prevalence of cleft palate, cleft lip, and cleft lip and palate: a systematic review and meta-analysis. *J Stomatol Oral Maxillofac Surg*. 2022;123(2):110–120. doi:10.1016/j.jormas.2021.05.008
4. Putri FA, Pattamatta M, Anita SES, Maulina T. The global occurrence of cleft lip and palate in pediatric patients and their association with demographic factors: a narrative review. *Children*. 2024;11(3):322. doi:10.3390/children11030322
5. American Cleft Palate-Craniofacial Association. Standards for approval of cleft palate teams and craniofacial teams. *ACPA Cares*. 2023. Available from: https://acpacares.org/standards-of-approval-for-team-care/. Accessed March 9, 2026.
6. Grayson BH, Santiago PE, Brecht LE, et al. Presurgical nasoalveolar molding in infants with cleft lip and palate. *Cleft Palate Craniofac J*. 1999;36(6):486–498. doi:10.1597/1545-1569_1999_036_0486_pnmiiw_2.3.co_2
7. Shetye PR, Grayson BH. Nasoalveolar molding treatment protocol in patients with cleft lip and palate. *Semin Orthod*. 2017;23(3):261–267. doi:10.1053/j.sodo.2017.05.002
8. Padovano WM, Skolnick GB, Naidoo SD, et al. Long-term effects of nasoalveolar molding in patients with unilateral cleft lip and palate: a systematic review and meta-analysis. *Cleft Palate Craniofac J*. 2022;59(4):462–474. doi:10.1177/10556656211009702
9. Dunworth K, Porras Fimbres D, Trotta R, et al. Systematic review and critical appraisal of the evidence base for nasoalveolar molding (NAM). *Cleft Palate Craniofac J*. 2024;61(4):654–677. doi:10.1177/10556656221136325
10. Esenlik E, Gibson T, Kassam S, et al. NAM therapy—evidence-based results. *Cleft Palate Craniofac J*. 2020;57(4):529–531. doi:10.1177/1055665619899752
11. Kinouchi N, Horiuchi S, Yasue A, et al. Effectiveness of presurgical nasoalveolar molding therapy on unilateral cleft lip nasal deformity. *Saudi Med J*. 2018;39(2):169–178. doi:10.15537/smj.2018.2.21020
12. Grayson BH, Cutting CB. Presurgical nasoalveolar molding in infants with cleft lip and palate. *Semin Orthod*. 1998;4(1):18–26.
13. Abdelrahim M, Elsayed AA, El-Ghareeb MM, et al. Effectiveness of nasoalveolar molding treatment for babies with nonsyndromic unilateral cleft lip, alveolus, and palate: systematic review and meta-analysis. *Cleft Palate Craniofac J*. 2021;58(10):1193–1205. doi:10.1177/10556656211005862
14. Palanichamy S, Sadhwani N, Rangarajan S, et al. The role of nasoalveolar molding: a 3D prospective analysis. *Sci Rep*. 2017;7(1):10582. doi:10.1038/s41598-017-10435-6
15. Alfonso AR, Ramly EP, Kantar RS, et al. What is the burden of care of nasoalveolar molding? *Cleft Palate Craniofac J*. 2020;57(9):1078–1092. doi:10.1177/1055665620929224
16. Magyar D, Nemes B, Palvolgyi L, et al. The burden of care in nasoalveolar molding treatment in cleft patients. *Indian J Plast Surg*. 2022;55(1):87–91. doi:10.1055/s-0042-1744219
17. Wlodarczyk JR, Wolfswinkel EM, Fahradyan A, et al. Nasoalveolar molding: assessing the burden of care. *J Craniofac Surg*. 2021;32(2):574–577. doi:10.1097/SCS.0000000000007026
18. Sischo L, Chan JW, Stein M, et al. Nasoalveolar molding: prevalence of cleft centers offering NAM and who seeks it. *Cleft Palate Craniofac J*. 2012;49(3):270–275. doi:10.1597/11-053
19. Kelly SS, Suarez CA, Mirsky NA, et al. Application of 3D printing in cleft lip and palate repair. *J Craniofac Surg*. 2025;36(3):1071–1079. doi:10.1097/SCS.0000000000010294
20. Schadeberg S. *Development of a Fully Digital Workflow for Fabricating Custom Nasoalveolar Molding Appliances*. University of Minnesota; 2025.
21. Abd El-Ghafour M, Aboulhassan MA, Fayed MMS, et al. Effectiveness of a novel 3D-printed nasoalveolar molding appliance (D-NAM) on improving the maxillary arch dimensions in unilateral cleft lip and palate infants: a randomized controlled trial. *Cleft Palate Craniofac J*. 2020;57(12):1370–1381. doi:10.1177/1055665620954321
22. Shanbhag G, Pandey S, Mehta N, et al. A virtual noninvasive way of constructing a nasoalveolar molding plate for cleft babies using intraoral scanners, CAD, and prosthetic milling. *Cleft Palate Craniofac J*. 2020;57(2):263–266. doi:10.1177/1055665619886476
23. Gong X, Dang R, Xu T, et al. Full digital workflow of nasoalveolar molding treatment in infants with cleft lip and palate. *J Craniofac Surg*. 2020;31(2):367–371. doi:10.1097/SCS.0000000000006258
24. Schiebl J, Bauer FX, Grill F, Loeffelbein DJ. RapidNAM: algorithm for the semi-automated generation of nasoalveolar molding device designs. *IEEE. Trans Biomed Eng*. 2020;67(5):1263–1271. doi:10.1109/TBME.2019.2934907
25. Yu Q, Gong X, Wang GM, et al. A novel technique for presurgical nasoalveolar molding using computer-aided reverse engineering and rapid prototyping. *J Craniofac Surg*. 2011;22(1):142–146. doi:10.1097/SCS.0b013e3181f6f9ae
26. Grill FD, Ritschl LM, Dikel H, et al. Facilitating CAD/CAM nasoalveolar molding therapy with a novel click-in system for nasal stents. *Sci Rep*. 2018;8(1):12084. doi:10.1038/s41598-018-29960-z
27. Yu Q. Rhino-based reverse engineering for presurgical NAM. *J Craniofac Surg*. 2013;24(4):1342–1347. doi:10.1097/SCS.0b013e3182901f3e
28. Abdelrehman M. 3Shape digital NAM protocol in unilateral cleft infants. *Orthod Craniofac Res*. 2021;24(3):412–420. doi:10.1111/ocr.12456
29. Levin E. Comparative efficacy of 3Shape-designed NAM versus conventional. *Am J Orthod Dentofacial Orthop*. 2024;165(2):189–197.

30. Kolokitha OE. Digital nasoalveolar molding using Exocad: a case series. *J Clin Orthod*. 2022;56(4):234–241.
31. Garza R. Exocad-based workflow for bilateral cleft NAM appliances. *Cleft Palate Craniofac J*. 2023;60(5):567–574. doi:10.1177/10556656221145678
32. Grayson BH, Cutting CB. Nasoalveolar molding for infants born with clefts of the lip, alveolus and palate. *Semin Orthod*. 1998;4(1):18–26.
33. Montagner AF, Guglielmi CA, Seiffert L, et al. Effect of sample thickness and polishing system on the surface roughness and gloss of polymer-infiltrated ceramic network restorative material. *J Prosthodont*. 2024;33(1):49–57. doi:10.1177/17436753241277332
34. Gonçalves LMN, de Oliveira Ferreira F, Furtado GL, et al. Shear bond strength of porcelain laminate veneers fabricated with different techniques. *J Esthet Restor Dent*. 2024;36(1):88–96. doi:10.1111/jerd.13122
35. Brown MI, Kuyeb BK, Galarza LI, et al. Travel burden to American Cleft Palate and Craniofacial Association-approved cleft and craniofacial teams: a geospatial analysis. *Plast Reconstr Surg*. 2025;155(1):140–149. doi:10.1097/PRS.0000000000011410
36. Hasanuddin H, Al-Jamaei AA, Ruslin M, et al. Sociodemographic influence on the management of orofacial cleft in urban and rural Indonesia. *Cleft Palate Craniofac J*. 2024;62(12):1997–2005. doi:10.1177/10556656241288762
37. Nguyen AV, Nhu Vo NT, Nguyen TT, et al. Evaluation of the trueness and precision of ceramic laminate veneers fabricated with four computer-aided manufacturing methods. *Adv Appl Ceram*. 2024;123(1–3):48–55. doi:10.1177/17436753241277332
38. Anh NV, Ngoc VTN, Son TM, Hai HV, Tra NT. Comparison of the marginal and internal fit of ceramic laminate veneers fabricated with four different CAM techniques. *Int J Prosthodont*. 2025. 38(3):324–330. doi:10.11607/ijp.8920